



Study of interaction of antimutagenic 1,4-dihydropyridine AV-153-Na with DNA-damaging molecules and its impact on DNA repair activity

Elina Leonova^{1,2}, Evita Rostoka^{1,2}, Sylvie Sauvaigo³, Larisa Baumanė², Turs Selga¹ and Nikolajs Sjakste^{1,2}

¹ Faculty of Medicine, University of Latvia, Riga, Latvia

² Latvian Institute of Organic Synthesis, Riga, Latvia

³ LXRepair, Grenoble, France

ABSTRACT

Background. 1,4-dihydropyridines (1,4-DHP) possesses important biochemical and pharmacological properties, including antioxidant and antimutagenic activities. It was shown that the antimutagenic 1,4-dihydropyridine AV-153-Na interacts with DNA. The aim of the current study was to test the capability of the compound to scavenge peroxyxynitrite and hydroxyl radical, to test intracellular distribution of the compound, and to assess the ability of the compound to modify the activity of DNA repair enzymes and to protect the DNA in living cells against peroxyxynitrite-induced damage.

Methods. Peroxyxynitrite decomposition was assayed by UV spectroscopy, hydroxyl radical scavenging—by EPR spectroscopy. DNA breakage was determined by the “comet method”, activity of DNA repair enzymes—using Glyco-SPOT and ExSy-SPOT assays. Intracellular distribution of the compound was studied by laser confocal scanning fluorescence microscopy. Fluorescence spectroscopy titration and circular dichroism spectroscopy were used to study interactions of the compound with human serum albumin.

Results. Some ability to scavenge hydroxyl radical by AV-153-Na was detected by the EPR method, but it turned out to be incapable of reacting chemically with peroxyxynitrite. However, AV-153-Na effectively decreased DNA damage produced by peroxyxynitrite in cultured HeLa cells. The Glyco-SPOT test essentially revealed an inhibition by AV-153-Na of the enzymes involved thymine glycol repair. Results with ExSy-SPOT chip indicate that AV-153-Na significantly stimulates excision/synthesis repair of 8-oxoguanine (8-oxoG), abasic sites (AP sites) and alkylated bases. Laser confocal scanning fluorescence microscopy demonstrated that within the cells AV-153-Na was found mostly in the cytoplasm; however, a stain in nucleolus was also detected. Binding to cytoplasmic structures might occur due to high affinity of the compound to proteins revealed by spectroscopical methods.

Discussion. Activation of DNA repair enzymes after binding to DNA appears to be the basis for the antimutagenic effects of AV-153-Na.

Submitted 18 October 2017

Accepted 22 March 2018

Published 25 April 2018

Corresponding author

Nikolajs Sjakste,
Nikolajs.Sjakste@lu.lv

Academic editor

Yegor Vassetzky

Additional Information and
Declarations can be found on
page 12

DOI 10.7717/peerj.4609

© Copyright

2018 Leonova et al.

Distributed under

Creative Commons CC-BY 4.0

OPEN ACCESS

Subjects Biophysics, Cell Biology, Molecular Biology

Keywords 1,4-dihydropyridines, AV-153-Na, DNA repair

INTRODUCTION

Synthetic derivatives of 1,4-dihydropyridine (1,4-DHPs) possess important biochemical and pharmacological properties. They show modulating activity on cardiovascular and neuronal processes as well as anticancer, genoprotective and radioprotective effects. In the present investigation we have focused our attention on a representative of the 1,4-DHP derivatives, which is considered to be “unusual”. These compounds are water-soluble molecules without the activity of blockers of calcium channels or with a very weak blocking activity. 1,4-DHPs of this group manifest different biological activities, including genome-protecting effects; for example, glutapyrone is an antineoplastic and anticlastogenic agent, antimutagen and enhancer of DNA repair (*Goncharova et al., 2001; Kuzhir, Dalivelia & Savina, 1999; Vartanian et al., 2004*). Our interests were focused on the compound AV-153-Na possessing antimutagenic activity and being an enhancer of DNA repair (*Ryabokon, Cieslar-Pobuda & Rzeszowska-Wolny, 2009; Ryabokon et al., 2008; Ryabokon et al., 2005; Ryabokon et al., 2009*). Recently, we have revealed the DNA binding capacity of this compound (*Buraka et al., 2014*). The aim of the current study was to test the DNA-protective capability of the compound in formerly unstudied systems, to test the ability of the compound to scavenge peroxynitrite and hydroxyl radical, and to assess the ability of the compound to modify the activity of DNA repair enzymes. To achieve these goals, the study was designed as follows. Firstly we have evaluated possibility of direct interaction of the compound with DNA-damaging agents, hydroxyl radical and peroxynitrite *in vitro*, in order to reveal the role of direct chemical interactions in antimutagenic activity of AV-153-Na. Further, possible impact of the AV-153-Na on the dynamics of DNA breakage in living cells, and activity of DNA repair enzymes was studied by means of single cell electrophoresis and functional repair assays (Glyco-SPOT and ExSy-SPOT assays).

MATERIALS AND METHODS

Chemicals

AV-153-Na and AV-154-Na were synthesized in the Laboratory of Membrane Active Compounds at the Latvian Institute of Organic Synthesis. Structures of the AV-153-Na and AV-154-Na are given in [Fig. 1](#); the synthesis of the compounds was performed essentially as described (*Dubur & Uldrikis, 1969*). Tris base, ferrous sulphate, 5,5-dimethylpyrrolidine-*N*-oxide (DMPO), Triton-X-100, human serum albumin (HSA), Na₂EDTA, LiCl, NaCl, CaCl₂ and other inorganic salts were purchased from Sigma-Aldrich (Taufkirchen, Germany). Peroxynitrite was synthesized as described by *Robinson & Beckman (2005)*.

Cell culture

HeLa cells (Biomedical Research and Study Centre, Riga, Latvia) were grown in DMEM + Glutamax™-I, F-12 Nut-Mix (1×) (Sigma-Aldrich, Taufkirchen, Germany) + 10% fetal bovine serum (Sigma-Aldrich, USA), at 37 °C in a humidified atmosphere containing 5% CO₂.

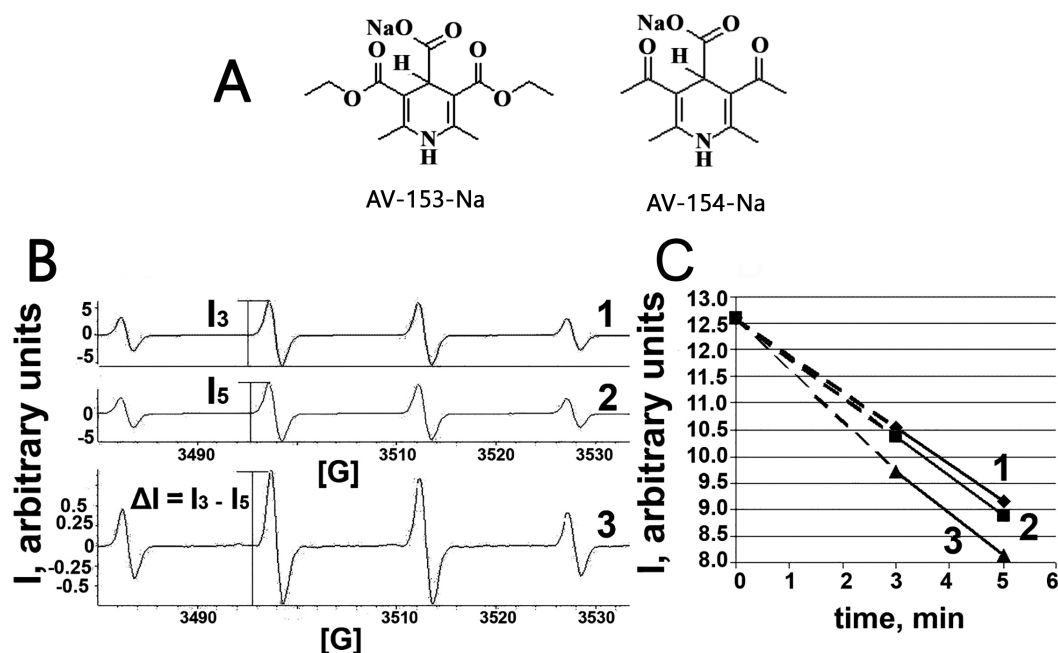


Figure 1 Electron paramagnetic resonance spectroscopy. (A) Chemical structures of AV-153 –Na and AV-154. (B) EPR spectra of DMPO-OH radicals generated in Fenton reaction in presence of DMPO. 1—EPR spectra of DMPO-OH radicals 3 min after mixing the components for Fenton reaction. 2—EPR spectra of DMPO-OH radicals 5 min after mixing the components for Fenton reaction. I₃ and I₅—intensities of EPR signals used for quantification of DMPO-OH radicals in corresponding time. 3—difference between 3 min and 5 min spectra indicating decrease of the signal intensity and lack of generation of other radicals. (C)—time course of decrease of intensity of DMPO-OH radical spectra. 1—control mixture; 2—in presence of AV-154-Na; 3—in presence of AV-153-Na.

Full-size [DOI: 10.7717/peerj.4609/fig-1](https://doi.org/10.7717/peerj.4609/fig-1)

Fenton reaction—ESR measurements

For the Fenton reaction ($\text{Fe}^{2+} + \text{H}_2\text{O}_2 \rightarrow \text{Fe}^{3+} + \cdot\text{OH} + \text{OH}^-$), 80 μl of reaction mixture containing 250 μM ferrous sulphate, 250 μM H_2O_2 , 80 mM spin trap DMPO, and 1 mM of 1,4 DHP was transferred to a micro pipettes tube for measurement of the electron spin resonance (ESR) spectra of DMPO-OH radicals. ESR spectra of the spin trap and radical complex were recorded at room temperature using an EMX-plus EPR spectrometer (Bruker, Germany). The EPR instrumental settings for field scan were as follows: field sweep—100G; microwave frequency—9.84 GHz; microwave power—15.9 mW; modulation amplitude—1 G; conversion time—163 ms; time constant—327 ms; sweep time—83 s; receiver gain— $1 \cdot 10^4$; resolution—512 points for 1 scan.

The single cell electrophoresis (comet assay)

The single cell electrophoresis (comet assay) was performed as described previously (Leonova et al., 2016)

UV/VIS spectroscopic measurement of peroxynitrite decomposition

The rate of peroxynitrite (0.38 mM) decomposition in the presence or in the absence of the 1,4-DHP (0.16 mM) was followed at 302 nm (absorbance peak for the peroxynitrite

anionic form) in 10 mM Tris pH 10 buffer on Perkin Elmer Lambda 25 UV/VIS spectrophotometer (Carballal, Bartesaghi & Radi, 2014). The average rate of reactions were calculated according to the formula $V = \pm((C_2 - C_1)/(t_2 - t_1)) = \pm(\Delta C/\Delta t)$, where C_1 was the concentration of peroxyxynitrite in the beginning of reaction, and C_2 the concentration of peroxyxynitrite at the end of the reaction; Δt : 20 min.

Circular dichroism spectroscopy

CD spectra were recorded on a Chirascan CS/3D spectrometer (Applied Photophysics, Surrey, UK); CD spectra of HSA in the absence or in the presence of AV-153-Na salts were recorded in PBS buffer, pH 7.4 in a range of 200–260 nm. A 300 nM HSA solution was titrated with AV-153-Na (1 μ M at each step) in a quartz cell of 10 mm path-length at room temperature. The parameters for the spectra were as follows: scan rate—200 nm min⁻¹, averaging time—0.125 s, bandwidth—1 nm; one recorded spectrum is the average of four scans.

Fluorescence spectroscopic measurements

Spectrofluorimetric analyses were performed on a Fluoromax-3 (Horiba JOBIN YVON, Shanghai, China), essentially as described (Osina et al., 2017).

Cell treatment and nuclear extract preparation for repair reactions

HeLa cells were incubated with 50 nM of AV-153-Na for 3, 12 or 24 h, washed with PBS, trypsinized, suspended in PBS and pelleted by low-speed centrifugation. Cell pellets were incubated in ice for 20 min in 1.25 mL of ice-cold buffer A (10 mM HEPES pH 7.9, 1.5 mM MgCl₂, 10 mM KCl, 0.01% Triton X-100, 0.5 mM DTT, 0.5 mM PMSF) and vortexed for 30 s. After centrifugation for 5 min at 5,000 rpm at 4 °C, the nuclei were suspended in 31.25 μ L of ice-cold buffer B (10 mM HEPES pH 7.9, 1.5 mM MgCl₂, 400 mM KCl, 0.2 mM EDTA, 25% glycerol, 0.5 mM DTT, antiproteases (Complete-mini, Roche, Meylan, France) and 0.5 mM PMSF). The nuclear membrane lysis was completed by incubation for 20 min on ice, followed by two cycles of freezing-thawing at -80 °C and 4 °C respectively. Debris was eliminated by centrifugation for 10 min at 13,000 rpm at 4 °C. The supernatant was stored frozen in 10 μ l aliquots at -80 °C. Protein content was determined using the BCA kit (Interchim, Montluçon, France). Typical protein content was 0.8 mg/mL.

Assays of the activity of DNA repair enzymes

The impact of the tested compounds on activity of glycosylases/AP endonucleases belonging to Base Excision Repair and on Excision/Synthesis Repair activities was performed using Glyco-SPOT (Pons et al., 2010) and ExSy-SPOT assays (Forestier et al., 2012), respectively (LXRepair, Grenoble, France). These assays allowed quantifying different DNA repair activities from extracts prepared from treated and non-treated cells.

The former chip, which is a multiplex, on-support, oligonucleotide (ODN) cleavage assay, reveals excision activities against 8-oxoguanine paired with C (8-oxoG-C), A paired with 8oxoguanine (A-8oxoG), ethenoadenine (EthA-T), thymine glycol (Tg-A), uracil (paired either with G or A (U-G and U-A, respectively)), hypoxanthine (Hx-T), and abasic sites (THF-A). Cleavage of the lesions by the enzymes contained in the extracts released the fluorescence attached to the lesion containing ODNs.

Repair reactions were conducted for 1 h at 37 °C with 15 µg/mL of protein in 80 µL of excision buffer (10 mM Hepes/KOH pH 7.8, 80 mM KCl, 1 mM EGTA, 0.1 mM ZnCl₂, 1 mM DTT, 0.5 mg/mL BSA). After 3 washes, 5 min at room temperature in PBS containing 0.2 M NaCl and 0.1% Tween 20, the spots fluorescence was quantified using the Innoscan scanner from Innopsys (Toulouse, France). Each extract was run in duplicate. The results between the replicates (4 spot fluorescence) were normalized using the NormalizeIt software as described by *Millau et al. (2008)*.

Wells incubated with the excision buffer served as reference (100% fluorescence) to calculate the lesions percentage of cleavage in the wells incubated with the extracts. Non-specific cleavage of the control ODN (Lesion_Free ODN) was also taken into account to calculate the percentage of excision of each lesion using the following formula: $(100 \times (1 - \text{percentage of fluorescence of Lesion_ODN} / \text{percentage of fluorescence of Lesion_Free ODN}))$.

The ExSy-SPOT assay quantified Excision/Synthesis Repair of 8-oxoguanine (8oxoG), alkylated bases (AlkB) and abasic sites (AbaS), incorporated into different supercoiled plasmid DNA. The principle of the methods is described by *Millau et al. (2008)*. Extracts (0.1 mg/mL) incubated on the biochip where the different plasmid preparations were immobilized at specific sites for 3 h at 30 °C in reaction buffer (40 mM Hepes KOH pH 7.8, 7 mM MgCl₂, 0.5 mM DTT, 0.25 µM dATP, 0.25 µM dTTP, 0.25 µM dGTP, 3.4% glycerol, 12.5 mM phosphocreatine (Sigma, Taufkirchen, Germany), 2 mM EDTA, 50 µg/mL creatine phosphokinase, 0.1 mg/mL BSA) containing 1 mM ATP (Amersham, England) and 1.25 µM dCTP-Cy3. After washing for 3 × 5 min in H₂O (MilliQ), the total fluorescence intensity of each spot was quantified using the Innoscan scanner from Innopsys (Toulouse, France). Each extract was run in duplicate and data were normalized using the NormalizeIt software as described by *Millau et al. (2008)*. Results were expressed as Fluorescence Intensity (FI).

Laser confocal scanning microscopy

For imaging, the HeLa cells were seeded in 4 well Nunc Lab-Tek Permanox Chamber slide (Thermo Scientific Nunc, Pittsburg, PA, USA) and cultivated for 24 h as described above. Subsequently, the cells were washed twice with PBS for 5 min and then incubated with 1 mM AV-153-Na in PBS for 16 h in a CO₂ incubator at 37 °C and 5% CO₂. After incubation, the cells were washed with PBS for 5 min and fixed in 70% ethanol for 0.5 h at room temperature. Slides were rinsed with PBS for 5 min and counterstain chromatin was dyed with 15 µM propidium iodide (PI) in PBS for 0.5 h, then washed twice with PBS for 5 min. Slides were analyzed using a Leica DM RA-2 microscope equipment with a TCS-SL confocal scanning head (Leica Microsystems, Bannockburn, IL, USA). Images were collected with a Leica 40× HCX PL Fluator objective (NA = 0.75) and 100× HCX PIAPO oil immersion objective (NA = 1.40). AV-153-Na and propidium iodide were excited with a 488 nm band from a four-line argon ion laser. AV-153-Na fluorescence was detected between 510 and 560 nm, propidium iodide fluorescence was detected between 600 and 650 nm. Cell shapes were controlled with reflected light 475–505 nm. Cells were scanned along the Z-axis with a step size—0.5 µm.

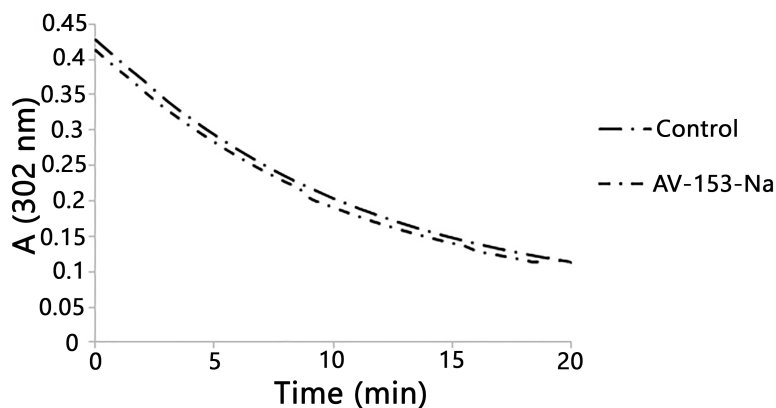


Figure 2 Reaction with peroxynitrite assay. Curves demonstrate decomposition of peroxynitrite (0.38 mM) in the presence of AV-153-Na added up to 0.16 mM at pH 10. The 1,4-DHP was added also to the control cuvette.

Full-size DOI: [10.7717/peerj.4609/fig-2](https://doi.org/10.7717/peerj.4609/fig-2)

Statistical analysis

The values of DNA damage assayed by single gel electrophoresis are represented as the mean \pm standard error of the mean (SEM). The data were subjected to the one-way analysis of variance (ANOVA), followed by the Tukey multiple comparisons test and the data were considered as significant at $p < 0.05$.

RESULTS

Study of chemical interactions of AV-153-Na with DNA-damaging agents

Taking into account capability of the AV-153-Na to decrease DNA damage produced by hydrogen peroxide (*Ryabokon et al., 2008; Ryabokon et al., 2005*) we have tested the ability of the AV-153-Na to scavenge free radicals. The OH radical produced in Fenton reaction, was tested by the ESR method. We have tested AV-153-Na at 1,000 μM concentration. The signals of the second component of the EPR spectra were measured on the 3rd min (I_3) and the 5th min (I_5) and the difference between I_3 and I_5 was calculated (*Fig. 1*). Scavengers of OH radicals should increase the difference between I_3 and I_5 . Representative kinetics of the decrease of EPR signal intensity is shown in *Fig. 1C*. The impact of AV-153-Na on the signal intensity is minimal, AV-154-Na does not produce any effect at all. Thus these 1,4-DHP derivatives are very weak radical scavengers.

Published data indicate the ability of some 1,4-DHP to scavenge peroxynitrite chemically (*Lopez-Alarcon et al., 2004*). We also tested the ability of the AV-153-Na salts to degrade peroxynitrite chemically by studying the kinetics of decomposition of peroxynitrite in the presence of DHP followed by means of spectrophotometry. The curves are presented in *Fig. 2*. The average rate of spontaneous decomposition of peroxynitrite at concentration 0.38 mM was 0.0157 $\mu\text{mol}/\mu\text{l min}$. AV-153-Na did not affect the time of decomposition of peroxynitrite; it remained 0.0157 $\mu\text{mol}/\mu\text{l min}$.

Intracellular localization of AV-153-Na and protein binding

As the capability of AV-153-Na to bind DNA *in vivo* was proven previously ([Buraka et al., 2014](#)), its antimutagenic effect could not be attributed to chemical interactions with DNA-damaging agents (see above) we needed evidence whether the compound could reach cell nucleus in the cells where it could interact with DNA. We have tried to answer this question by profiting of the intrinsic fluorescence of the compound with the aid of laser confocal scanning microscopy. Results are presented in [Figs. 3A](#) and [3C](#). In most cells AV-153-Na heavily stains the cytoplasm; however, some fluorescence is visible also in the nucleus, mainly in the nucleolus. Staining of cytoplasmic structures raised the question about capability of the compound to bind proteins. Fluorescence titration of AV-153-Na with human serum albumin gave a positive answer to the question - fluorescence of the compound increased in the presence of HSA. Results of CD confirmed the ability to bind a protein ([Figs. 3D](#) and [3E](#)). The addition of the compound to the HSA solution decreased CD signals in both minimal bands (208 and 222 nm) in the presence of AV-153-Na, which suggests binding with HSA, causing protein conformational changes due to a slight protein unfolding ([Wang et al., 2008](#)).

Impact of AV-153-Na on DNA damage and DNA repair systems

The DNA-protecting action of AV-153 salts against peroxyxynitrite-induced damage was tested in living cells. Results of the comet assay experiments performed on HeLa cell treated with peroxyxynitrite alone or in the presence of AV-153-Na are presented in [Fig. 4](#). Treatment with peroxyxynitrite drastically increased the levels of DNA damage. AV-153-Na reduced the extent of DNA damage produced by peroxyxynitrite. Pre-incubation with the compound at concentrations 50 nM for 45 min appeared to produce significant effects ([Fig. 4A](#)). When administered simultaneously with peroxyxynitrite, the compound produced a much weaker protective effect. AV-154-Na, which does not bind DNA ([E Leonova et al., 2018](#), unpublished data), did not protect the cells against peroxyxynitrite ([Fig. 4C](#)).

Effects of AV-153-Na on the activity of DNA repair enzymes were tested using Glyco-SPOT and ExSy-SPOT assays. Longer pre-incubation times were chosen to reveal possible changes in protein expression.

The Glyco-SPOT assay revealed a specific and significant decrease of Tg (thymine glycol) repair by AV-153-Na, which manifested itself when an extract with a higher concentration of protein (15 $\mu\text{g/ml}$) was used in the assay, and a trend for inhibition of enzymes involved in U-G and U-A repair ([Fig. 5](#)). Other glycosylases/AP endonucleases activities were not affected.

Results with ExSy-SPOT assay appear to be more interesting in this sense. AV-153-Na stimulates the excision/synthesis repair of lesions repaired by Base Excision Repair (8-oxoG, abasic sites and alkylated bases ([Fig. 6](#))). As this stimulating effect is not detected with the Glyco-SPOT assay, it involves either the synthesis step of the repair process or alternative repair pathways able to handle oxidative lesions.

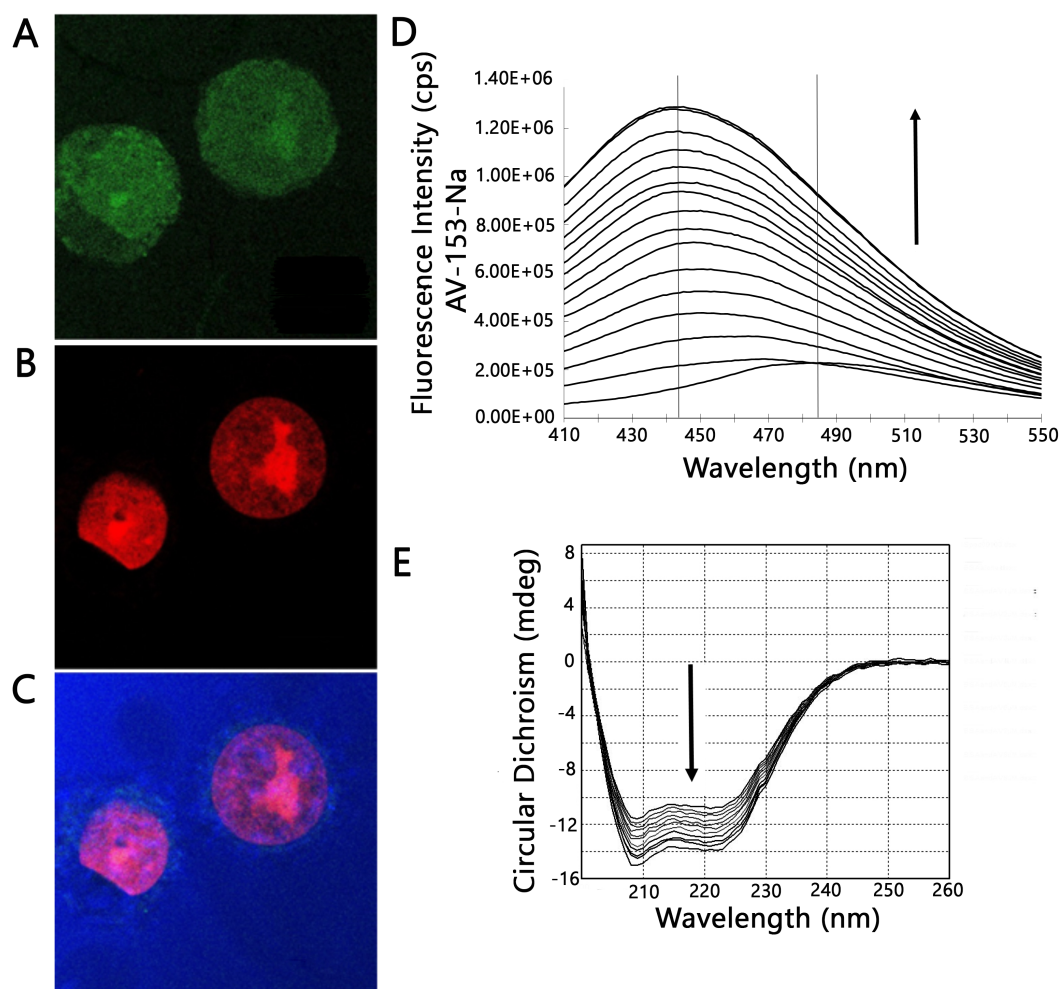


Figure 3 Confocal microscopy and protein binding assay. (A–C) images of HeLa cells obtained by laser scanning confocal microscopy. Cells were treated with AV-153-Na, DNA was stained with propidium iodide (PI). Light blue—reflected light; (A) green—distribution of AV-153-Na; (B) red—propidium iodide; the overlay image (C) of all channels. Pictures of the optical section were taken 3 μm from the cell surface. All the scale bars are in 7.5 μm size. (D) Fluorescence titration of AV-153-Na with human serum albumin (5 μM each time). (E) Circular dichroism spectra of HSA in absence and presence of AV-153-Na. AV-153-Na concentration was increased by 1 μM at each step up to 12 μM . HSA concentration was 300 nM.

Full-size DOI: [10.7717/peerj.4609/fig-3](https://doi.org/10.7717/peerj.4609/fig-3)

DISCUSSION

In order to test if the antimutagenic effects of the AV-153-Na are due to its capability to scavenge free radicals and peroxyntirite, we have studied these effects using *in vitro* systems, as some 1,4-DHP are able to scavenge different reactive oxygen and nitrogen species themselves; the reactions can be observed *in vitro* (Pacheco et al., 2013; Vijesh et al., 2011). Unexpectedly, it turned out that the compound does not react with peroxyntirite, and ability to scavenge hydroxyl radical turned out to be modest, thus the cause of the antimutagenic effect should have been sought inside the cells. We report evidence of

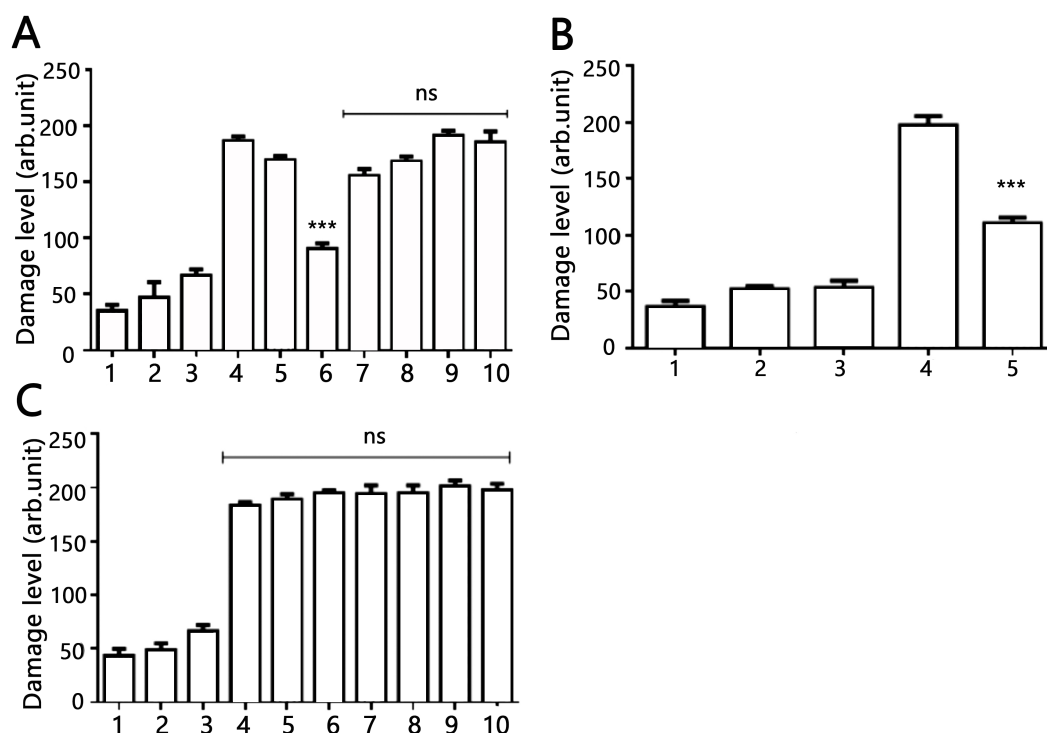


Figure 4 Effects of AV-153-Na and AV-154-Na against peroxyxynitrite caused DNA damage in HeLa cell line tested by comet assay. (A) AV-153-Na. 1, control (intact cells); 2, vehicle control (60 μ M of NaOH); 3, peroxyxynitrite (200 μ M); 4, incubation with the tested 1,4-DHP (100 nM, 45 min), 5, pre-incubation with 10 nm of 1,4-DHP (45 min) and treatment with peroxyxynitrite; 6, pre-incubation with 50 nm of 1,4-DHP (45 min) and treatment with peroxyxynitrite; 7, pre-incubation with 100 nm of 1,4-DHP (45 min) and treatment with peroxyxynitrite; 8, simultaneous treatment with 1,4-DHP (10 nm) and peroxyxynitrite; 9, simultaneous treatment with 1,4-DHP (50 nM) and peroxyxynitrite; 10, simultaneous treatment with 1,4-DHP (100 nM) and peroxyxynitrite; (B) AV-153-Na. 1, control (intact cells); 2, incubation with 50 nM of AV-153-Na for 3 h; 3, vehicle control (60 μ M of NaOH; 3 h); 4, peroxyxynitrite (200 μ M); 5, pre-incubation with 50 nm of AV-153-Na (3 h) and treatment with peroxyxynitrite; (C) AV-154-Na, all designations are as in A. *** - $p < 0.001$ versus peroxyxynitrite group, ns, not significant.

Full-size DOI: [10.7717/peerj.4609/fig-4](https://doi.org/10.7717/peerj.4609/fig-4)

possible binding of the AV-153-Na to cell nucleus. Thus the DNA-binding activity of the compound could be responsible for its antimutagenic activity.

However, binding to DNA is usually considered to be mutagenic, this might seem to be in contradiction with its reported antimutagenic and DNA-protecting activities of the compound (Goncharova et al., 2001; Ryabokon, Cieslar-Pobuda & Rzeszowska-Wolny, 2009; Ryabokon et al., 2008; Ryabokon et al., 2005; Ryabokon et al., 2009). In contradiction to this point of view, analysis of literature data reveals the coexistence of DNA-binding activity with antimutagenic effects. Natural polyphenols provide a good illustration of this statement: many of them effectively bind DNA through intercalation; however, most of these compounds are considered to be antimutagenic. The latter activity is attributed to antioxidant properties of this class of compounds (Janjua et al., 2009; Zhang et al., 2011). It appears that the DNA-damaging and DNA-protecting activities cohabitate in the molecules of flavonoids. Even better example is presented by widely used antidiabetic

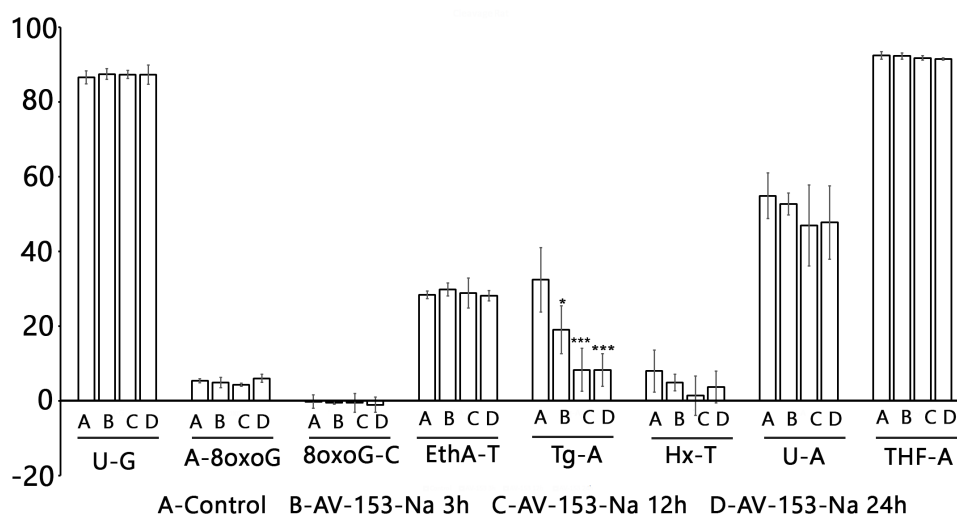


Figure 5 Effect of AV-153-Na on cellular Base Excision Repair activities (Glyco-SPOT assay). The test was run with 15 $\mu\text{g/ml}$ of extract prepared from non-treated cells (Control) and cells treated for 3 h, 12 h and 24 h with AV-153-Na as described in Materials and Methods. Results are expressed as cleavage rate for each lesion. U-G and U-A : uracil paired either with G or with A; A-8oxoG: A paired with 8oxoguanine; 8oxoG-C: 8-oxoguanine paired with C; EthA-T ethenoadenine paired with T; Tg-A : thymine glycol paired with A; Hx-T : hypoxanthine paired with T; THF-A : abasic sites analogue paired with A. * $p < 0.05$, *** $p < 0.001$ versus Tg-A control.

Full-size DOI: [10.7717/peerj.4609/fig-5](https://doi.org/10.7717/peerj.4609/fig-5)

drug metformin. It protects the type 2 *diabetes mellitus* patients from cancer development (Safe, Nair & Karki, 2018), it protects DNA against breakage (Algire et al., 2012), it interferes with efficiency of the DNA repair (Lee et al., 2016) but it binds the DNA (Shahabadi & Heidari, 2012).

Data of comet assay when the AV-153-Na was tested for ability to modify level of DNA breakage in HeLa cells exposed to peroxynitrite provide more evidence for the role of the DNA binding in the mutagenic effect of the compound. Pre-incubation with AV-153-Na significantly decreased the DNA damage. Perhaps a higher efficiency of low concentrations of AV-153-Na reflects a shift of the equilibrium between DNA damage being a consequence of DNA-binding and DNA protection towards DNA protection. The necessity for pre-incubation and lower efficiency of simultaneous administration with peroxynitrite indicates that AV-153-Na induces some changes in the cells favouring protection of DNA or DNA repair, as the compound does not interact directly with the peroxynitrite. Moreover, the good DNA binder AV-153-Na was an effective DNA protecting agent, while AV-154-Na, which does not interact with DNA at all, did not protect it against peroxynitrite. It seems that data on the impact of AV-153-Na on the activity of the excision repair enzymes makes understanding of the mechanism of action of the compound possible. AV-153-Na activates enzymes involved in the excision repair pathway. The observed decrease in Tg removal produced by AV 153-Na apparently contradicts data about DNA-protecting effects of the compound. However, it should be taken into account that in mammals two bifunctional glycosylases, NTH1 and NEIL1, show overlapping activities aimed on the removal of Tg (Sampath, 2014). Our data do not permit us to determine which enzyme was inhibited.

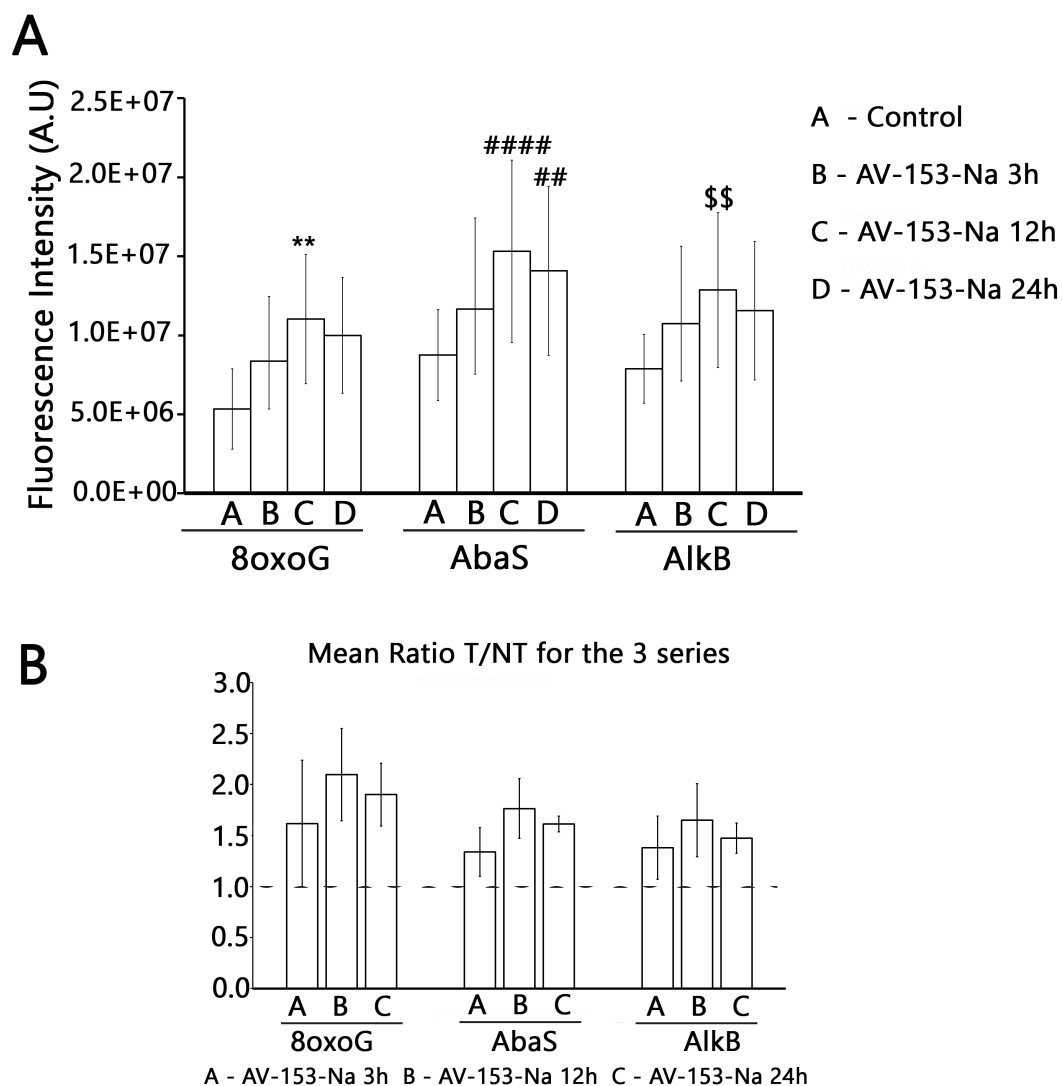


Figure 6 Effect of AV-153-Na on cellular Excision/Synthesis Repair (ExSy-SPOT assay) of major base lesions. The repair reaction was conducted with nuclear extracts prepared from non-treated cells and cells treated for 3 h, 12 h and 24 h with AV-153-Na (see Materials and Methods). For each lesion, we calculated the ratio of the fluorescence intensity obtained with the treated cells over the fluorescence intensity obtained with the control cells. The values > 1 reflect an induction of the Excision/Synthesis Repair activities. ** $p < 0.01$ versus 8oxoG control; ##### $p < 0.0001$ versus AbaS control; * $p < 0.01$ versus AlkB control.

Full-size DOI: [10.7717/peerj.4609/fig-6](https://doi.org/10.7717/peerj.4609/fig-6)

Although this finding cannot explain the DNA-protecting effects of AV-153-Na, it appears to be interesting.

The study further reveals binding to cytoplasmic structures and a high affinity to proteins. It might happen that cytoplasmic proteins retain the main part of AV-153-Na molecules after exposure of the cells to the compound; only a small part of the molecules reaches DNA, where these activate DNA repair systems but do not produce harmful effects due to a very low local concentration in the nucleus.

Summarizing the data, it can be proposed that binding of the compound to DNA is identified by DNA repair systems as DNA lesions, and activity of DNA repair systems is increased. It seems that AV-153-Na *per se* does not induce mutations; however, it triggers the the activity of DNA repair enzymes, thus making cells less vulnerable by other mutagens.

CONCLUSIONS

AV-153-Na protects the cells against genotoxic action of peroxyxynitrite although it does not react with peroxyxynitrite chemically. The protective effect is probably achieved due to direct interactions of the AV-153-Na with DNA and following activation of the DNA excision repair enzymes.

ACKNOWLEDGEMENTS

We thank U Kalnenieks and R Rutkis (Institute of Microbiology and Biotechnology of the University of Latvia) for giving access to their equipment.

ADDITIONAL INFORMATION AND DECLARATIONS

Funding

The work was supported by the State Research Program “Biomedicine 2014” and ECO-NET RUS programme project “DNA Parylation”. Collaboration between the Latvian and French teams was supported by the “Osmose” program. The funders had no role in study design, data collection and analysis, decision to publish, or preparation of the manuscript.

Grant Disclosures

The following grant information was disclosed by the authors:
Biomedicine 2014.
DNA Parylation.
Osmose program.

Competing Interests

Sylvie Sauvaigo is an employee of LXRepair, Grenoble, France, a private company.

Author Contributions

- Elina Leonova and Evita Rostoka conceived and designed the experiments, performed the experiments, analyzed the data, prepared figures and/or tables, authored or reviewed drafts of the paper, approved the final draft.
- Sylvie Sauvaigo and Larisa Baumane conceived and designed the experiments, performed the experiments, analyzed the data, contributed reagents/materials/analysis tools, authored or reviewed drafts of the paper, approved the final draft.
- Turs Selga conceived and designed the experiments, analyzed the data, contributed reagents/materials/analysis tools, prepared figures and/or tables, authored or reviewed drafts of the paper, approved the final draft.

- Nikolajs Sjakste conceived and designed the experiments, analyzed the data, prepared figures and/or tables, authored or reviewed drafts of the paper, approved the final draft.

Data Availability

The following information was supplied regarding data availability:

The raw data are provided in the [Supplemental File](#).

Supplemental Information

Supplemental information for this article can be found online at <http://dx.doi.org/10.7717/peerj.4609#supplemental-information>.

REFERENCES

- Algire C, Moiseeva O, Deschênes-Simard X, Amrein L, Petruccelli L, Birman E, Viollet B, Ferbeyre G, Pollak MN. 2012.** Metformin reduces endogenous reactive oxygen species and associated DNA damage. *Cancer Prevention Research* 5:536–543 DOI 10.1158/1940-6207.capr-11-0536.
- Buraka E, Chen CY, Gavare M, Grube M, Makarenkova G, Nikolajeva V, Bisenieks I, Bruvere I, Bisenieks E, Duburs G, Sjakste N. 2014.** DNA-binding studies of AV-153, an antimutagenic and DNA repair-stimulating derivative of 1,4-dihydropyridine. *Chemico-Biological Interactions* 220:200–207 DOI 10.1016/j.cbi.2014.06.027.
- Carballal S, Bartesaghi S, Radi R. 2014.** “Kinetic and mechanistic considerations to assess the biological fate of peroxyxynitrite”. *Biochimica et Biophysica Acta/General Subjects* 1840(2):768–780 DOI 10.1016/j.bbagen.2013.07.005.
- Dubur GYA, Uldrikis YAR. 1969.** Preparation of 3,5-diethoxycarbonyl-2,6-dimethyl-1,4-dihydroisonicotinic acid and 3,5-diacetyl-2,6-dimethyl-1,4-dihydroisonicotinic acid and their salts. *Khimiya Geterociklicheskikh Soedinenii* 5(6):1015–1017 (In Russian).
- Forestier A, Sarrazy F, Caillat S, Vandenbrouck Y, Sauvaigo S. 2012.** Functional DNA repair signature of cancer cell lines exposed to a set of cytotoxic anticancer drugs using a multiplexed enzymatic repair assay on biochip. *PLOS ONE* 7:e51754 DOI 10.1371/journal.pone.0051754.
- Goncharova R, Zabrejko S, Dalivelya O, Kuzhir T. 2001.** Anticlastogenicity of two derivatives of 1,4-dihydroisonicotinic acid in mouse micronucleus test. *Mutation Research/Genetic Toxicology and Environmental Mutagenesis* 496:129–135 DOI 10.1016/S1383-5718(01)00223-6.
- Janjua NK, Siddiq A, Yaqub A, Sabahat S, Qureshi R, Ul Haque S. 2009.** Spectrophotometric analysis of flavonoid-DNA binding interactions at physiological conditions. *Spectrochimica Acta Part A Molecular and Biomolecular Spectroscopy* 74:1135–1137 DOI 10.1016/j.saa.2009.09.022.
- Kuzhir TD, Dalivelia OV, Savina NV. 1999.** Modification of the repair processes in chemical mutagenesis in *Drosophila melanogaster*. *Genetika* 35:919–924.
- Lee YS, Doonan BB, Wu JM, Hsieh TC. 2016.** Combined metformin and resveratrol confers protection against UVC-induced DNA damage in A549 lung cancer

- cells via modulation of cell cycle checkpoints and DNA repair. *Oncology Reports* 35:3735–3741 DOI 10.3892/or.2016.4740.
- Leonova E, Sokolovska J, Boucher JL, Isajevs S, Rostoka E, Baumane L, Sjakste T, Sjakste N. 2016.** New 1,4-Dihydropyridines down-regulate nitric oxide in animals with streptozotocin-induced diabetes mellitus and protect deoxyribonucleic acid against peroxy nitrite action. *Basic & Clinical Pharmacology & Toxicology* 119:19–31 DOI 10.1111/bcpt.12542.
- Lopez-Alarcon C, Speisky H, Squella JA, Olea-Azar C, Camargo C, Nunez-Vergara LJ. 2004.** Reactivity of 1,4-dihydropyridines toward SIN-1-derived peroxy nitrite. *Pharmaceutical Research* 21:1750–1757 DOI 10.1023/B:PHAM.0000045224.97323.8b.
- Millau JF, Raffin AL, Caillat S, Claudet C, Arras G, Ugolin N, Douki T, Ravanat JL, Breton J, Oddos T, Dumontet C, Sarasin A, Chevillard S, Favier A, Sauvaigo S. 2008.** A microarray to measure repair of damaged plasmids by cell lysates. *Lab Chip* 8:1713–1722 DOI 10.1039/b806634e.
- Osina K, Leonova E, Isajevs S, Baumane L, Rostoka E, Sjakste T, Bisenieks E, Duburs G, Vigante B, Sjakste N. 2017.** Modifications of expression of genes and proteins involved in DNA repair and nitric oxide metabolism by carbanionides [disodium-2,6-dimethyl-1,4-dihydropyridine-3,5-bis(carboxyloxyacetate) derivatives] in intact and diabetic rats. *Arhiv za Higijenu Rada I Toksikologiju* 68:212–227 DOI 10.1515/aiht-2017-68-2945.
- Pacheco SR, Braga TC, Da Silva DL, Horta LP, Reis FS, Ruiz AL, De Carvalho JE, Modolo LV, De Fatima A. 2013.** Biological activities of eco-friendly synthesized Hantzsch adducts. *Med Chem* 9:889–896 DOI 10.2174/1573406411309060014.
- Pons B, Belmont AS, Masson-Genteuil G, Chapuis V, Oddos T, Sauvaigo S. 2010.** Age-associated modifications of Base Excision Repair activities in human skin fibroblast extracts. *Mechanisms of Ageing and Development* 131:661–665 DOI 10.1016/j.mad.2010.09.002.
- Robinson KM, Beckman JS. 2005.** Synthesis of peroxy nitrite from nitrite and hydrogen peroxide. *Methods in Enzymology* 396:207–214 DOI 10.1016/s0076-6879(05)96019-9.
- Ryabokon NI, Cieslar-Pobuda A, Rzeszowska-Wolny J. 2009.** Inhibition of poly(ADP-ribose) polymerase activity affects its subcellular localization and DNA strand break rejoining. *Acta Biochimica Polonica* 56:243–248.
- Ryabokon NI, Goncharova RI, Duburs G, Hancock R, Rzeszowska-Wolny J. 2008.** Changes in poly(ADP-ribose) level modulate the kinetics of DNA strand break rejoining. *Mutation Research/DNA Repair* 637:173–181 DOI 10.1016/j.mrfmmm.2007.08.005.
- Ryabokon NI, Goncharova RI, Duburs G, Rzeszowska-Wolny J. 2005.** A 1,4-dihydropyridine derivative reduces DNA damage and stimulates DNA repair in human cells in vitro. *Mutation Research/DNA Repair* 587:52–58 DOI 10.1016/j.mrgentox.2005.07.009.
- Ryabokon NI, Nikitchenko NV, Dalivelya OV, Goncharova RI, Duburs G, Konopacka M, Rzeszowska-Wolny J. 2009.** Modulation of cellular defense processes in human

- lymphocytes in vitro by a 1,4-dihydropyridine derivative. *Mutation Research/DNA Repair* **679**:33–38 DOI [10.1016/j.mrgentox.2009.07.010](https://doi.org/10.1016/j.mrgentox.2009.07.010).
- Safe S, Nair V, Karki K. 2018.** Metformin-induced anticancer activities: recent insights. *Biological Chemistry* **399**(4):321–335 DOI [10.1515/hsz-2017-0271](https://doi.org/10.1515/hsz-2017-0271).
- Sampath H. 2014.** Oxidative DNA damage in disease—insights gained from base excision repair glycosylase-deficient mouse models. *Environmental and Molecular Mutagenesis* **55**:689–703 DOI [10.1002/em.21886](https://doi.org/10.1002/em.21886).
- Shahabadi N, Heidari L. 2012.** Binding studies of the antidiabetic drug, metformin to calf thymus DNA using multispectroscopic methods. *Spectrochimica Acta Part A Molecular and Biomolecular Spectroscopy* **97**:406–410 DOI [10.1016/j.saa.2012.06.044](https://doi.org/10.1016/j.saa.2012.06.044).
- Vartanian LP, Ivanov EV, Vershinina SF, Markochev AB, Bisenieks EA, Gornaeva GF, Iu IPustovalov, Ponomareva TV. 2004.** Antineoplastic effect of glutapyrone in continual gamma-irradiation of rats. *Radiatsionnaia Biologiya, Radioecologia* **44**:198–201.
- Vijesh AM, Isloor AM, Peethambar SK, Shivananda KN, Arulmoli T, Isloor NA. 2011.** Hantzsch reaction: synthesis and characterization of some new 1,4-dihydropyridine derivatives as potent antimicrobial and antioxidant agents. *European Journal of Medicinal Chemistry* **46**:5591–5597 DOI [10.1016/j.ejmech.2011.09.026](https://doi.org/10.1016/j.ejmech.2011.09.026).
- Wang N, Ye L, Yan F, Xu R. 2008.** Spectroscopic studies on the interaction of azelnidipine with bovine serum albumin. *International Journal of Pharmaceutics* **351**:55–60 DOI [10.1016/j.ijpharm.2007.09.016](https://doi.org/10.1016/j.ijpharm.2007.09.016).
- Zhang S, Sun X, Jing Z, Qu F. 2011.** Spectroscopic analysis on the resveratrol-DNA binding interactions at physiological pH. *Spectrochimica Acta Part A Molecular and Biomolecular Spectroscopy* **82**:213–216 DOI [10.1016/j.saa.2011.07.037](https://doi.org/10.1016/j.saa.2011.07.037).